Marine Pollution Bulletin 187 (2023) 114501

Contents lists available at ScienceDirect

Marine Pollution Bulletin

journal homepage: www.elsevier.com/locate/marpolbul

Baseline

Baseline concentrations, spatial distribution and origin of trace elements in marine surface sediments of the northern Antarctic Peninsula

Louise J. Delhaye [a,*], Marc Elskens [b], Constanza Ricaurte-Villota [c], Luis Cerpa [d], Marc Kochzius [a]

[a] Marine Biology, Ecology & Biodiversity, Vrije Universiteit Brussel (VUB), 1050 Brussels, Belgium
[b] Analytical, Environmental and Geo-Chemistry Laboratory, Vrije Universiteit Brussel (VUB), 1050 Brussels, Belgium
[c] Program of Marine and Coastal Geosciences, Institute of Marine and Coastal Research (INVEMAR), Santa Marta, Colombia
[d] Instituto Geológico Minero y Metalúrgico (INGEMMET), Lima, Peru

ARTICLE INFO

Keywords:
Trace metals
ICP-MS
FP-XRF
Southern Ocean
Contamination

ABSTRACT

Increased human activity in the Antarctic Peninsula combined with accelerated melting of its glaciers highlights the importance of monitoring trace element concentrations. Surface sediment samples were collected around King George Island, Hope Bay and in the Bransfield Strait in February 2020 and were analysed by X-ray fluorescence spectroscopy and inductively coupled plasma mass spectrometry. The methods display a good correlation. Our results show clear distinctions between these regions for selected elements with high local heterogeneities. Hope Bay exhibited lower concentrations of Fe, Mn, Co, V, Zn while most stations in the Bransfield Strait and around King George Island showed moderate to significant enrichment in Cu, As and Cd. Twelve stations presented a moderate ecological risk. The consistency of our values supports a natural rather than anthropogenic origin, possibly related to volcanism and the geology of the area. However, our results suggest an increase in Cr that should be further investigated.

Long-range atmospheric and oceanic currents have brought anthropogenic pollutants to Antarctica since the industrial revolution. More recently, the intensification of human activity on and around the continent, combined with global warming, has raised new concerns about local increases in contaminants in this remote environment (Suttie and Wolff, 1993; Boutron et al., 1994; Bargagli, 2008; Vodopivez et al., 2015; Cabrita et al., 2017; Reed et al., 2018). In particular, trace metals pose a potential ecological risk for the Antarctic ecosystem due to their persistent toxicity and their capacity to be bioaccumulated by organisms and biomagnified through the trophic chain. Evidence of such mechanisms have already been found in Antarctica and particularly around King George Island (KGI) (Santos et al., 2006; Trevizani et al., 2016; Webb et al., 2020).

The North-Western Antarctic Peninsula (NWAP) is the most visited part of the continent and, as such, deserves more attention. The NWAP is limited to the West by a chain of islands (i.e. the South Shetland Islands (SSI)) which are separated from the Antarctic Peninsula by the Bransfield Strait. Glaciers of this region experience high rates of melting and an associated increased glacial erosion is therefore expected in the coming years (Ribeiro et al., 2011; Barbosa et al., 2020; Webb et al., 2020). Given the geological characteristics of the SSI, this could potentially lead to an increase of trace metals in the sediments (Farías et al., 2007; Ribeiro et al., 2011). The Antarctic Treaty and the creation of an Antarctic Specially Managed Area in Admiralty Bay (KGI) demonstrate the importance of protecting these areas. For these reasons, several authors recommend establishing baseline concentration levels of trace elements in order to allow adequate monitoring (Ahn et al., 1996; Bargagli, 2000; Gasparon and Matschullat, 2006; Trevizani et al., 2018). However, this can only be achieved by using consistent and reliable measurement methods whose results are comparable in space and time. Field-portable X-ray fluorescence (FP-XRF) is a commonly used method for in situ soil characterisation, promising rapid field screening of contaminated sites (IAEA, 2005), but is so far limited for trace element analysis due to relatively low sensitivity and accuracy (Bosneaga et al.,

Abbreviations: ICP-MS, Inductively coupled plasma mass spectrometry; FP-XRF, Field portable X-ray fluorescence spectrometry; KGI, King George Island; DI, Deception Island; NWAP, North-Western Antarctic Peninsula; SSI, South Shetland Islands; BS, Bransfield Strait; WBB, West Bransfield Basin; CBB, Central Bransfield Basin; CDW, Circumpolar Deep Water; CRM, Certified Reference Material; EF, Enrichment Factor; Igeo, Geo-accumulation Index; RI, Ecological Risk Index.

* Corresponding author at: Operational Directorate Natural Environment, Royal Belgian Institute of Natural Sciences (RBINS), Vautierstraat 29, 1000 Brussels, Belgium.

E-mail address: ldelhaye@naturalsciences.be (L.J. Delhaye).

https://doi.org/10.1016/j.marpolbul.2022.114501
Received 25 July 2022; Received in revised form 7 December 2022; Accepted 14 December 2022
Available online 28 December 2022
0025-326X/

2011). Therefore, sediment samples were also analysed by inductively coupled plasma mass spectrometry (ICP-MS). Properties, such as high sensitivity (ppt-ppq), relative salt tolerance, compound-independent elemental response, and accuracy, make ICP-MS an undeniable tool for efficient detection, identification, and quantification of trace elements (Ammann, 2007). In this study, 31 stations were sampled around KGI, in the Bransfield Strait and in Hope Bay (Fig. 1) and trace element concentrations in the surface sediments were measured using both FP-XRF and ICP-MS. Besides establishing baseline values, the objectives of this study were to (1) compare the results obtained by FP-XRF and ICP-MS, (2) uncover and understand the spatial distribution and origins of these elements and (3) compare the concentrations with published values from the scientific literature.

The Bransfield Strait (BS) is a narrow passage between the SSI and the northern part of the Antarctic Peninsula. It constitutes a semi-enclosed basin of about 55,000 km^2 (Gordon and Nowlin, 1977; Masqué et al., 2002). The BS basin is composed of three sub-basins with significantly different morphological and oceanographic characteristics (Gordon and Nowlin, 1977), separated from each other by narrow and relatively shallow (about 500 m deep) sills. In the current study, only two basins were sampled: the West Bransfield Basin (WBB), located to the South and West of Deception Island (DI), which has a maximum depth of 1000 m, and the Central Bransfield Basin (CBB), situated along KGI, which has a maximum depth of 2000 m (Bárcena et al., 2002). A line of both subaerial and submerged volcanic phenomena passes through the axis of the Strait (aerial or submarine volcanism, seamounts (e.g. the Orca seamount), calderas (DI), neovolcanic ridges or cinder cones, hydrothermal vents) (Smellie et al., 1984; Keller et al., 1991; Somoza et al., 2004). The BS is also distinguished by the complexity of its crust whose thickness varies significantly over the region and whose structure and composition are very heterogeneous (Biryol et al., 2018). The water masses within the basin consist of dense shelf water from the Weddell Sea to the East, Transitional Zonal Water with Bellingshausen influence to the West and modified circumpolar deep water (CDW) in the deeper parts of the basin (Veny et al., 2022). King George Island, part of the South Shetland archipelago, is the most populated island of the Antarctic Peninsula, with eight scientific bases and an airport. Admiralty Bay, comprising three scientific stations, is the largest bay of the island and was established as an “Antarctic Specially Protected Area” in 2006. It has also been classified as a site of prime importance for birds by BirdLife International. According to Islam and Tanaka (2004), contamination is increasing in the bay due to the growth in scientific and touristic activities. However, the level and origin of pollution in this area is disputed: while some authors found higher concentrations of trace metals near the stations (Ribeiro et al., 2011; Vodopivez et al., 2015; Trevizani et al., 2016), others suggest that the levels are equivalent to the upper crust or baseline values and would therefore not originate from anthropogenic sources (Santos et al., 2007; Vodopivez et al., 2019). This disagreement underlines the importance of conducting more in-depth studies in this area.

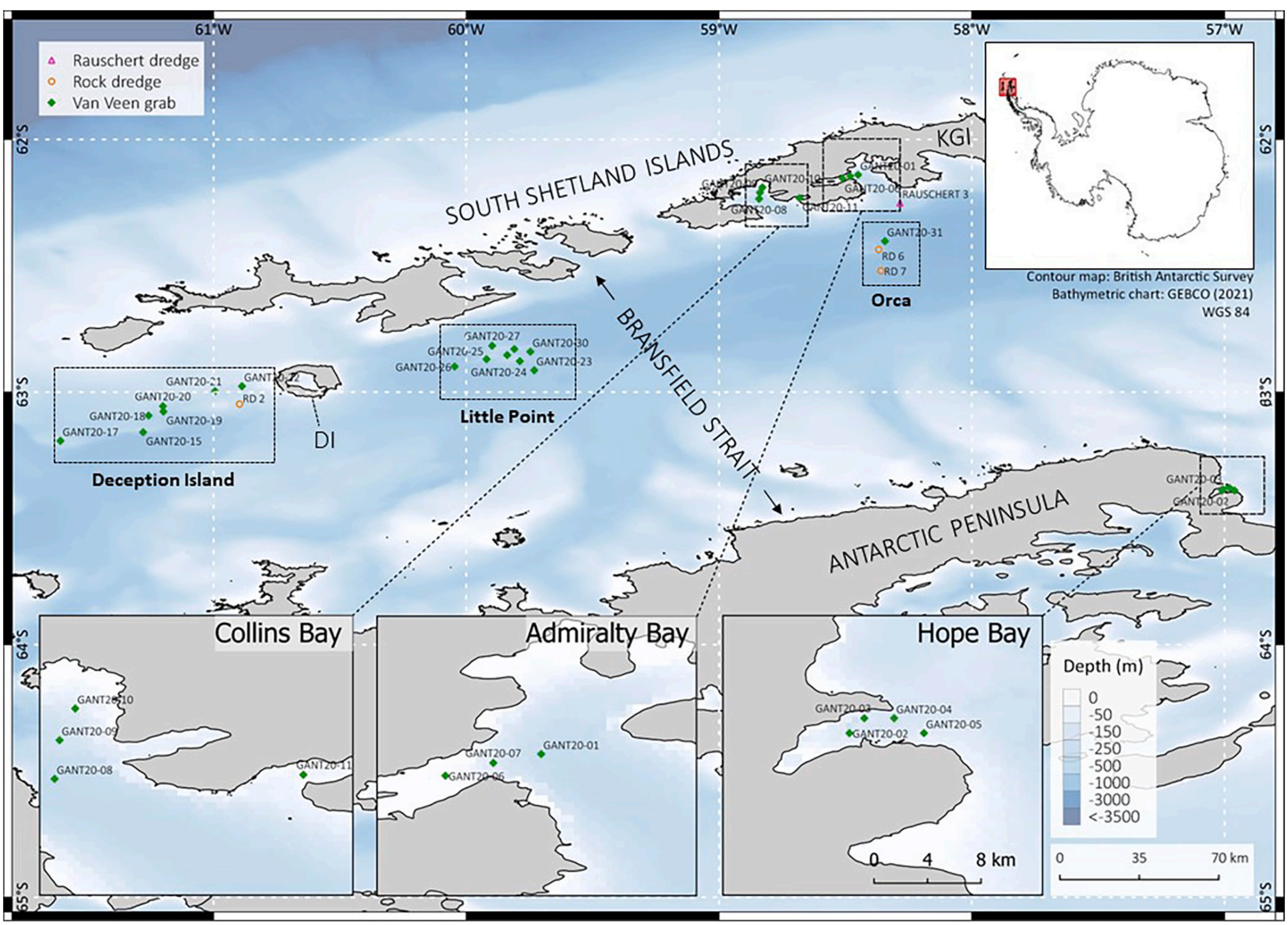

Fig. 1. Sampling stations around KGI, in Hope Bay and in the Bransfield Strait (Antarctica) where surface sediment samples were collected for trace element analyses using different equipment's (green diamond: Van Veen grab; orange circle: rock dredge; violet triangle: Rauschert dredge). The square on the map of Antarctica at the top right of the figure indicates the location of the study area. KGI = King George Island, DI = Deception Island. (For interpretation of the references to colour in this figure legend, the reader is referred to the web version of this article.)

In this study, samples were taken during the second leg of the 27th expedition of Peru to Antarctica (ANTARXXVII) on board the BAP Carrasco, in February 2020. Surface sediments were collected for ICP-MS analysis at 28 stations using a Van Veen grab and both rock (RD) and Rauschert dredges (Table 1S, Fig. 1). From each sample, 100 g of sediments were taken using plastic tools to avoid any contamination and directly stored in plastic bottles. These had been decontaminated with diluted HCl prior to the campaign and transported in closed plastic bags. The samples were directly placed at −20 °C before the sediments were dried on board at 45 °C in an oven for a minimum of 24 h. The dried sediments were then partially crushed and placed in zip bags. Between each sample, the tools were thoroughly rinsed with MilliQ water.

Prior to the ICP-MS analyses, small portions of the collected sediment samples were freeze dried in the home laboratory. A microwave-assisted digestion method was used to determine the overall trace metal concentrations in these freeze-dried soils according to Gao et al. (2013). First, 0.10 to 0.15 g of the sediment samples were transferred to a digestion vessel. Three solutions were then added: 4 ml of 40 % suprapure concentrated HF, 6 ml of distilled concentrated nitric acid (65 %) and 2 ml of concentrated HCl (37 %). The vessels were then closed and placed in the microwave for 10 min at 180 °C. After cooling, 30 ml of 4 % H_3BO_3 was added before the solution was heated to 120 °C for 10 min in a microwave following the standard method EPA 3052. To validate the sample extraction procedure (homogenisation, weighing and digestion), procedural blank, working standard, solutions, drift control samples, and certified reference material (CRM), whose target element concentrations of Al, As, Cd, Co, Cr, Cu, Fe, Hg, Mn, Ni, Pb, V, Zn are known were used. In the current study, this CRM, whose matrix is close to the matrix of the sample to be analysed was MESS-3 Marine Sediment Reference Materials for Trace Metals and other Constituents provided by the National Research Council of Canada. This CRM allowed testing the recovery during the extraction procedure (accuracy) and precision under repeatability conditions (Table 1).

Except for Fe, the recovery values (accuracy) for all the measured elements were between 80 and 120 %, which corresponds to the usual acceptable deviation limits (Thompson et al., 2002). For precision, two sets of conditions are relevant: (a) precision under repeatability conditions describing the variations observed during a single series of measurements and (b) precision under run-to-run conditions (within-laboratory reproducibility). The two uncertainty sources act on individual analytical results, which therefore have a combined value. Both estimates are obtained by analysing the selected test sediment from GANT20-15 in duplicate in seven successive runs. The separate variance components are then calculated by applying a one-way analysis of variance (Thompson et al., 2002). Each duplicate analysis was an independent execution of the whole extraction procedure applied to a separate sample portion. The expected precision under repeatability conditions varied between 1 and 7 %, while the precision under run-to run conditions ranges between 3 and 12 %. The latter being slightly higher than those measured under repeatability conditions, suggesting that the samples taken with the Van Veen grab after drying and grinding were rather homogeneous.

During the same cruise, samples for FP-XRF analysis were collected with a Van Veen grab at 20 stations. Sediment samples of 7.35 cm^3 were extracted and placed in plastic containers. Before proceeding to the X-ray spectrum analysis, each container was wrapped with plastic foil in order to avoid contact with the scanner system. X-ray fluorescence spectroscopy was performed immediately after collection, without prior manipulation, using a FP-XRF analyser (Bruker XRF Tracer Series IV-SD). The samples were placed directly on the emitting lens, with a 60 s detection time. Every measurement consisted of two successive phases; the first phase operated at 45 kV/15 μA and the second at 15 kV/45 μA. Each sample was measured three times, the average of these technical replicates was calculated and PPM concentrations measured for 20 elements (i.e. As, Ca, Co, Cr, Cu, Fe, Mn, Mo, Nb, Ni, Pb, Rb, Sb, Sn, Sr, Th, Ti, Y, Zn, and Zr). The variability between the replicates for each element was calculated in three steps: 1) for each sampling station, the sum of the absolute values of the replicates' deviations from the mean was divided by the number of replicates, 2) the mean deviation was then divided by the mean and multiplied by 100 and 3) the percentage of deviation for each station was averaged for each element. The results (Table 2) showed a high variability between consecutive measurements of the same sample for Cr (41 %) and Ni (30 %). Data obtained from the analyses were compared with the tables of quantification limits for the calibration of Mudrock Trace, obtained from Drake (2014). The counting error varied between 70 and 90 % depending on the element. The concentrations measured by ICP-MS and FP-XRF at each station are shown in the Supplementary Materials (Tables 2S and 3S).

The basis for interpretation of FP-XRF data involves consideration of signals from the sample, instrument artefacts and physical phenomena. XRF spectra allow for a qualitative and possibly semi-quantitative interpretation of the data. To this end, we cross-referenced them with the ICP-MS results through Deming regressions in R using the mcr package. The Pearson correlation coefficient was >0.97 with a p-value of <0.0001. The slope of the regression line (95%CI: 0.40–1.31) was not significantly different from 1 (Fig. 2A). Comparing the results by means of box plots (Fig. 2B), a satisfactory match between the FP-XRF and ICP-MS results was observed for As, Co, Cr, Cu, Fe, Mn, Ni, Pb and Zn. Of the nine elements measured by both FP-XRF and ICP-MS, most showed a significant positive correlation ($p \leq 0.05$) (Fig. 1S). Overall, the FP-XRFs estimates tended to be slightly underestimated compared to ICP-MS ones with slope values ranging from 0.26 to 0.96. For As, Cr and Zn, the slope of the Deming regression line was not different from zero at the 5 % significance level. This suggests that in this study it would be possible to use FP-XRF data in a semi-quantitative way for trace metal screening in surface sediments.

After a robust statistical analysis for the determination of outliers according to Daszykowski et al. (2007), it was considered that the Hg value determined by ICP-MS for GANT20-06 was an extreme non-representative value for the analysed data series. To avoid bias in further calculations (PCA and pairwise comparisons), it was decided to correct this value by the mean of the two contiguous stations (GANT20-01 and GANT20-07) (i.e. 0.0265 μg/g). In order to meet the second objective of this study (i.e. uncover and understand the spatial distribution and origins of the trace elements), multiple statistical tests were executed in Python and R. Firstly, a multiple factor analysis (MFA) (Fig. 3) was performed on the two datasets (FP-XRF and ICP-MS) and revealed a clear geochemical distinction between the different areas. The sample GANT20-11, located in Potter Cove, was considered part of Collins Bay for the purpose of the MFA since it is located in the same area of KGI. To confirm these observations, pairwise statistical tests between each zone were performed on the ICP-MS data. An ANOVA test followed by a Tukey test was used, or, in case that the condition of normality of the data was not met, a Kruskal-Wallis and a Dunn's test (Table 4S) were performed. The results indicated that the stations in Hope Bay were significantly different from the rest of the study area, having lower

Table 1
Accuracy and precision for the ICP-MS measurements of surface sediment samples.

	Al	As	Cd	Co	Cr	Cu	Fe	Hg	Mn	Ni	Pb	V	Zn
Recovery %	84	110	106	100	91	96	63	100	100	98	102	105	87
Repeatability %	2	3	7	2	2	4	2	3	3	1	3	2	4
Within laboratory reproducibility %	5	11	12	5	3	5	3	11	4	6	3	3	4

Table 2
Inter-replicates variability (%) of FP-XRF data for each trace element.

	As	Ca	Co	Cr	Cu	Fe	Mn	Mo	Nb	Ni	Pb	Rb	Sb	Sn	Sr	Th	Ti	Y	Zn	Zr
Inter-replicates variability %	9	5	7	41	18	4	4	9	13	30	7	8	6	10	5	5	6	4	7	7

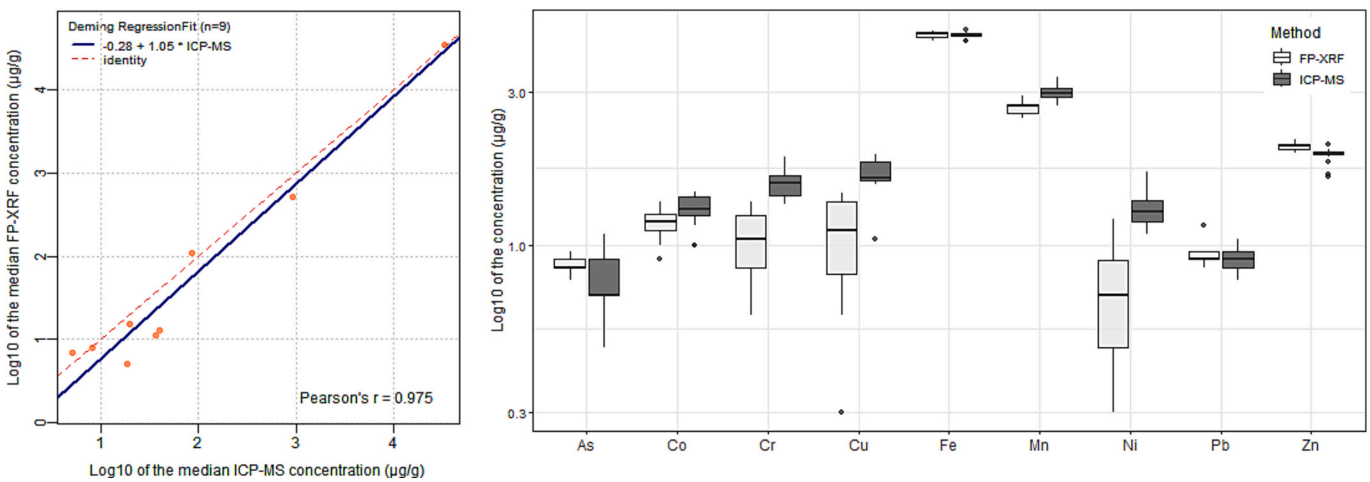

Fig. 2. Deming regression between the median concentrations (µg/g) (left, panel A) and boxplots of the concentrations (µg/g) (right, panel B) of As, Co, Cr, Cu, Fe, Mn, Ni, Pb and Zn measured by FP-XRF and ICP-MS.

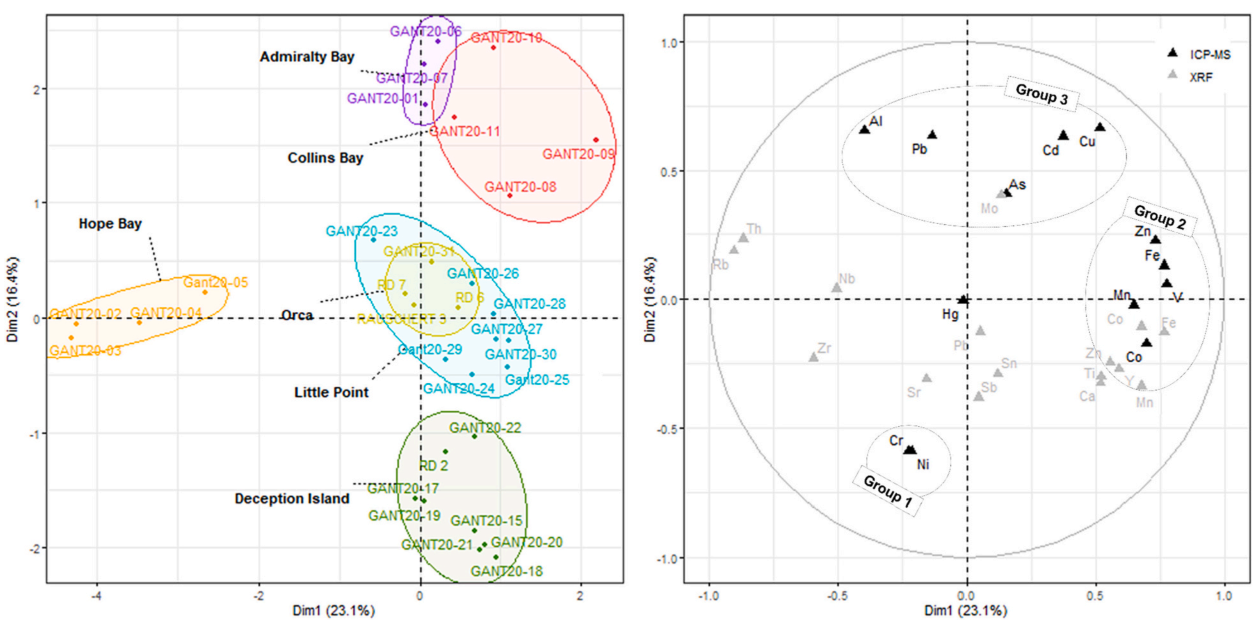

Fig. 3. Multiple Factors Analysis (left, panel A) and correlation circle (right, panel B) of the concentrations of trace elements in surface sediments measured by FP-XRF and ICP-MS for each sampling station around King George Island, in Hope Bay and in the Bransfield Strait. On panel B, sub-circles show the three groups of elements established according to the ICP-MS results. (For interpretation of the references to colour in this figure legend, the reader is referred to the web version of this article.)

concentrations of Fe, Mn, Co, V and Zn than most other locations. A similar geological distinction has been observed in other studies (Castillo et al., 2014; Simões et al., 2018). On the right-hand side of the MFA (Fig. 3A), the other stations are spread out in a vertical gradient, reflecting the spatial distribution of the samples and the varying tectonic and lithological environment. The stations West of Deception Island, in the WBB, are found at the bottom of the graph (Fig. 3A), followed by the stations at Orca and Little Point (CBB) and finally the stations around KGI are located at the top of the graph. With regard to the latter, while the stations of Admiralty Bay are relatively similar to each other, there seems to be a higher heterogeneity among the stations of Collins Bay. Around KGI, stations generally have higher concentrations of Al, As, Cd, Cu, Pb in the sediments, most of these trace elements are considered toxic for organisms. On the opposite, stations in the WBB have higher concentrations of Cr and Ni. Based on this MFA, it was possible to group the samples into four areas with geochemically distinct surface sediments: KGI, DI, the CBB (Orca and Little Point) and Hope Bay. This distinction between DI and KGI (Penguin Island) was also noted by Guerra et al. (2011). However, in our study, we found opposite results, with higher Cr, V and Ni concentrations around DI. This geochemical distinction was used in order to better understand the regional origin of trace elements using detailed MFAs and Spearman rank correlations (Figs. 4 and 2S).

Fig. 3B shows the correlations among the different elements and with the principal components of the MFA. The Spearman rank correlation revealed several significant correlations between the different elements (Fig. 2S) which were consistent with those observed on Fig. 3B. On this basis, the elements were categorised into three groups: (1) Ni and Cr, (2) Co, Fe, Mn, Zn and V and (3) Cu, Cd, As, Pb and Al. Within each group, elements present a similar spatial distribution (Fig. 5) although these correlations vary at the regional level (Figs. 4 and 2S).

The first group includes Ni and Cr, which are positively correlated with each other ($r = 0.89$, $p \leq 0.001$), but negatively correlated with Cu and As. These last two elements are naturally present in high concentrations in the environment of the BS due to the geology of the region (Ribeiro et al., 2011; Guerra et al., 2011; Farías et al., 2007). A significant negative correlation between Cr and As was also found in the sediments of Admiralty Bay by Santos et al. (2007) and suggests that Ni and Cr would come from a non-erosive origin, contrary to the findings of Ahn et al. (1996), Andrade et al. (1999) and Guerra et al. (2011). The later study suggests the presence of Cr-rich minerals in the rocks of Penguin Island (KGI) as an explanation for the relatively high Cr concentrations in the sediments. Ni values over the entire study area and Cr values at DI are negatively correlated with Cd.

The second group is composed of Co, Fe, Mn, V and Zn. Except for Co and Zn, the five elements of this group are all strongly positively

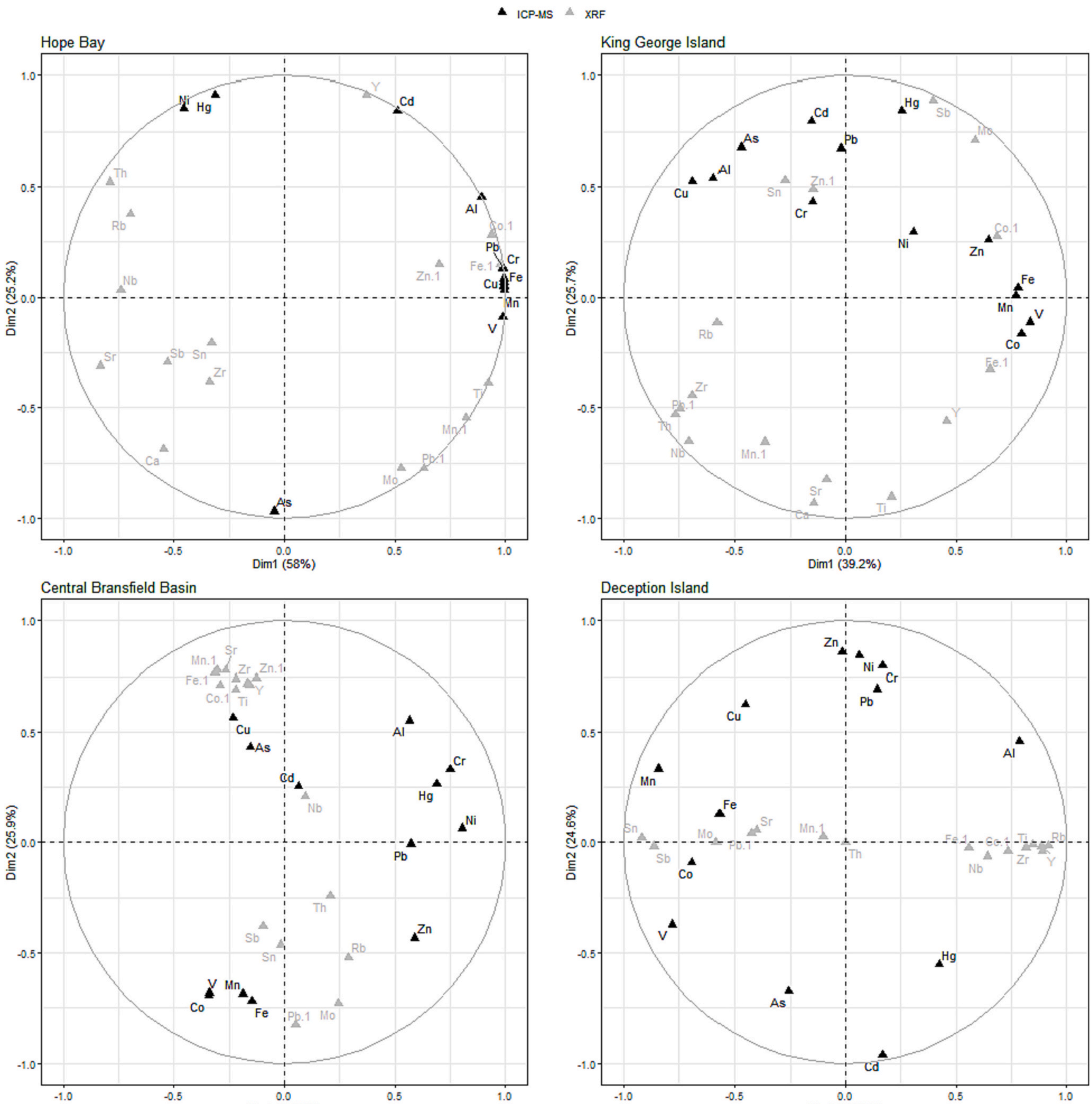

Fig. 4. Correlation circles of the concentrations of trace elements in surface sediments measured by FP-XRF and ICP-MS for every geochemical area (Hope Bay, King George Island, Central Bransfield Basin and Deception Island).

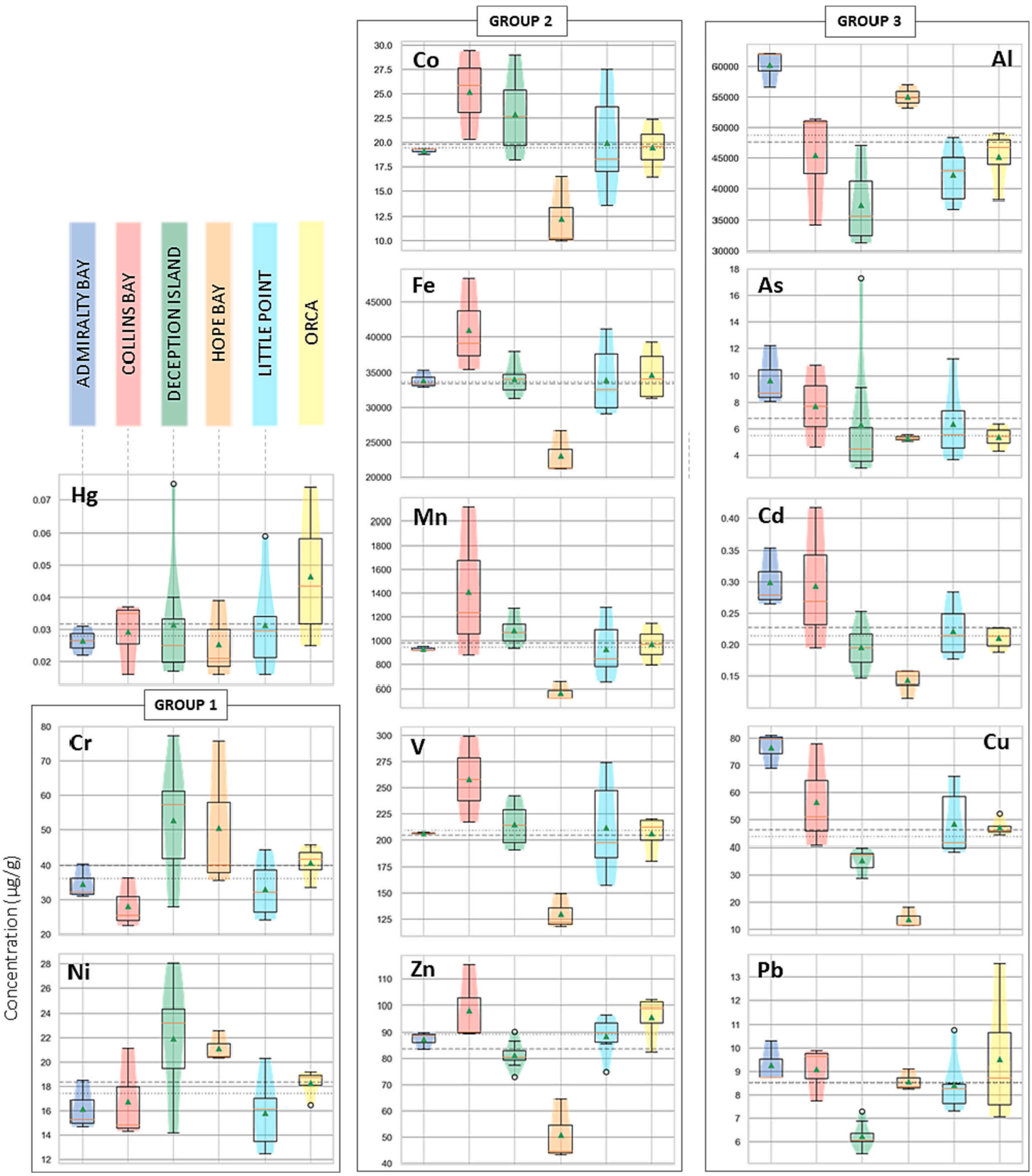

Fig. 5. Boxplots of the trace elements measured by ICP-MS for each area (from left to right: violet: Admiralty Bay; red: Collins Bay; green: Deception Island; orange: Hope Bay; blue: Little Point; yellow: Orca). The wide grey band in the background behind the boxplots indicates the average profile of each group. (For interpretation of the references to colour in this figure legend, the reader is referred to the web version of this article.)

correlated with each other (Fig. 2S). Contrary to the findings of Ahn et al. (2004) for element particulate concentrations in seawater, we found a significant negative correlation between Al and Mn, V, Co, Fe in marine surface sediments, suggesting that they would have a non-erosive origin. In their study, however, they concluded that these elements were linked to glacial melt-water input in Admiralty Bay. Ahn et al. (2004) also found a positive correlation between Zn and Cu while in our study, although these two elements showed a significant positive correlation at the level of the study area ($r = 0.40$, $p = 0.05$), they displayed a significant negative correlation in Admiralty Bay ($r = -0.857$, $p = 0.05$). Our results are also opposite to those found by Trevizani et al. (2016) who found high Zn and Cu concentrations around Admiralty Bay and explained it as being a product of erosion of basaltic andesite present on the island. Furthermore, Zn was found to be positively correlated with depth ($r = 0.49$; $p = 0.01$), suggesting it was present in higher concentrations at deeper stations, perhaps because of hydrothermal activity.

The third group contains most of the toxic elements (i.e. As, Cd, Cu, Pb and Al). Cu, Cd and As, all naturally present in high concentrations in the environment around KGI (Ahn et al., 1996; Vodopivez et al., 2001; Farías et al., 2007; Ribeiro et al., 2011), are correlated with each other. Pb is positively correlated with Al and appears to be the only element of group 3 occurring in notable quantities in the geology of Hope Bay. Indeed, in Fig. 4, it can be seen that all elements of this group follow the same spatial distribution as Al for all areas except Hope Bay. While erosion appears to be as high as in Admiralty Bay (similar Al concentrations), the concentrations of As, Cd and Cu are comparatively much lower. The only trace element negatively correlated with depth is As ($r = -0.42$, p = 0.05), which is consistent with the hypothesis that it originates from erosion. The latter process, intensified by climate change and increased glacial runoff, might lead to a higher contribution of elements of erosive origins in shallow marine sediments.

Correlations between Hg and other elements are only visible when looking at the regional level (Fig. 2S). The main distinction between Orca and Little Point (CBB) is the higher concentration of Hg present in the sediments of Orca (Fig. 5), which is comparatively higher than in the other areas. This could be explained by the proximity of hydrothermal activities. However, our values are much lower than those found at the direct proximity of such vents (0.034–0.074 μg/g in Orca for this study compared to 0.29–114 μg/g in hydrothermal sediments from other studies (Lee et al., 2015)).

The enrichment factor (EF) and geo-accumulation index (Igeo) are two indicators widely used for evaluating the potential anthropogenic contamination of surface sediments. For EF, the concentrations of trace elements were normalised with Al. Background values from the upper continental crust were taken from Wedepohl (1995). The values for the enrichment factor were then classified in five categories from deficiency (EF < 2) to extremely high enrichment (EF > 40). The Igeo was classified in seven categories from uncontaminated (Igeo < 0) to extremely contaminated (Igeo > 5) (Barbieri, 2016). The ecological risk index (RI) was calculated as the sum of all the contamination values for a specific element (CF) multiplied by the toxicity of that element. Values were then categorised from low ecological risk (RI < 150) to very high ecological risk (RI > 600) (Hakanson, 1979). The toxicity equivalency factors (TEF) for each element were taken from Kuerban et al. (2020) (i.e.: Hg = 40; Cd = 30; As = 10; Cu = Ni = Pb = 5; Cr = 2 and Zn = 1). Results are presented in Table 5S of the Supplementary Materials.

$$\mathrm{EF} = (\mathrm{Cm}/\mathrm{CAl})_{\mathrm{sample}} \Big/ (\mathrm{Cm}/\mathrm{CAl})_{\mathrm{background}} \tag{1}$$

where Cm is the concentration of the metal and CAl is the concentration of Al

$$\mathrm{Igeo} = \log 2\left(\mathrm{Cm}_{\mathrm{sample}} / 1.5^{*}\mathrm{Cm}_{\mathrm{background}}\right) \tag{2}$$

$$\begin{aligned} \mathrm{RI} &= \sum (\mathrm{TEF}^{*}\mathrm{CF}) \text{ where} \\ \mathrm{CF} &= \mathrm{Cm}_{\mathrm{sample}} / \mathrm{Cm}_{\mathrm{background}} \end{aligned} \tag{3}$$

Almost all stations in the Bransfield Strait and around KGI were significantly enriched in As and Cu compared to the average trend of the earth's crust (Table 5S). In contrast, Hope Bay showed moderate EF values for As and even a deficit for Cu. High Cu concentrations are not surprising around King George Island and have been previously discussed by Ribeiro et al. (2011). Glacial erosion of magmatic rocks (mainly basalt-andesite) and frequent chalcopyrite mineralisation in the region are proposed as probable causes of the high Cu concentrations. The presence of andesite in the sediments was visually reported at several stations in this study. High As values were also recorded close to Arctowski station on KGI by Ribeiro et al. (2011), although at lower concentrations than the values obtained in our study. High As values were believed to be caused by the maintenance operations needed for the research station. However, we found a significant enrichment of As at most sampling stations, suggesting that these consistent As and Cu enrichments are both more suggestive of a geological and mineralogical setting rich in these two elements than of external contamination. This hypothesis is supported by the study of Farías et al. (2007), who also found high values of As in the sediments of Potter Cove and explained them by the presence of the Barton Horst, the central tectonic block forming the island, where minerals containing As (such as arsenopyrite, SFeAs) are present. Based on the geo-accumulation index, fifteen stations were moderately contaminated with As or Cu, mainly around KGI and a few stations at Little Point and Orca (Table 5). Special attention should be given to stations GANT20-06 and GANT20-22, which showed higher As concentrations than most stations (respectively 12 μg/g and 17 μg/g) and were considered as moderately to heavily contaminated. Cd showed a moderate enrichment for all sampling stations except for GANT20-03, in Hope Bay, where values were deficient and GANT20-10 and RD 2 which both showed significant enrichment. High Cd concentrations in Antarctic coastal waters would be linked to the upwelling of the CDW (Bargagli et al., 1996, Ianni et al., 2010; Vodopivez et al., 2015, Webb et al., 2020). In our study, Cd and As were significantly correlated with each other ($r = 0.63$, $p \leq 0.001$), suggesting that Cd would more likely originate from erosion and meltwater input. Potapowicz et al. (2020) found Cd enrichment in multiple terrestrial sediment samples around Admiralty Bay, citing petroleum and wastewater disposal as potential sources of this element. Stations GANT20-06 and GANT20-10 were moderately contaminated with Cd as derived from the geo-accumulation index. Stations RD 2 and RD 7 were the only two stations with moderate Hg enrichment, and are both located near volcanic activities (DI, Orca seamount). All stations were in deficit with respect to Pb and most stations of DI were moderately enriched in Cr. Six of them were moderately enriched in Ni and one (GANT20-21) displayed a significant enrichment in Ni. This was also the case for RD 7, RAUSCHERT 2, GANT20-23 and GANT20-04. The distinction between Hope Bay and the rest of the study area was further confirmed by the results of Zn, which showed moderate enrichment everywhere except for Hope Bay (deficit) and two other stations: GANT20-01 and GANT20-11. Over the entire study area, the three elements mostly enriched at every station were Cd, As and Cu (Fig. 3S). A total of twelve stations showed a moderate ecological risk, including all three stations sampled in Admiralty Bay and two in Collins Bay. This ecological risk is owing to the naturally high presence of Cd, As and Cu in the environment around KGI. The two stations with the highest index (GANT20-06, GANT20-10) are both the innermost stations of the bays and could possibly be more influenced by erosion. The moderate ecological risk found for other stations could be explained by the presence of volcanic activities in the Bransfield Strait.

The third objective of this study (i.e. comparing the concentrations with the ones previously published in literature) is summarised in Table 3.

In Admiralty Bay, we found concentrations of Mn and Ni that were higher than previously measured. Concentrations of Mn, Fe and Zn in Collins Bay were also higher than those measured by Ahn et al. (1996) in 1993. In general, Mn concentrations in our study area were higher than measured at other sites around Antarctica except for the Ross Sea where most trace element concentrations are comparable. In contrast, the Weddell Sea has higher Cd, Cr and Ni concentrations. Most of the trace elements displayed values similar to those obtained in previous studies for Potter Cove since 1994. The influence of meltwater inputs, such as the Matías Creek discharge, would explain the high variability in the Fe values measured in Potter Cove (Vodopivez et al., 2015). The presence of high local heterogeneity around KGI is also emphasised by De Castro-Fernández et al. (2021) and Ahn et al. (2004). Pb concentration in our study was higher than measured in 1994–1995, 2005–2006 as well as most of the measurements made by Curtosi et al. (2010) in 2004–2005. However, in their study, they found two stations with clear

Table 3
Trace element concentration ranges in surface sediments measured in this study (in bold) compared to results of other studies in the same area and in other sites around Antarctica.

	As	*Cd*	*Co*	*Cr*	*Cu*	*Fe*	*Hg*	*Mn*	*Ni*	*Pb*	*Zn*
Admiralty Bay											
2002–2003[a]	–	–	–	31–35	67–92	–	–	527–624	7.9–10.1	5.5–10.5	52–89
2003[b]	–	<0.38	–	–	62.7	–	0.016–0.030	–	–	–	5.6–62.5
2004[c]	5.47–16.63	–	16.86–22.34	20.02–38.84	–	49,199–54,616	–	–	–	–	90.29–104.87
2006–2007[d]	2–12	0.4–0.9	–	7–12	47–84	–	–	–	3–10	3–11	44–89
2020[v]	**8.07-12.21**	**0.265-0.354**	**18.77–19.36**	**31.03–40.35**	**69.9–81.1**	**32,892–35,317**	**0.022–0.031**	**918–951**	**15.68–18.50**	**8.74–10.31**	**83.55–89.78**
Collins Bay											
1993[e]	–	0.22	18	7.6	77	24,200	–	640	15.4	8.7	69
2020[v]	**4.63-10.81**	**0.195-0.417**	**20.29–29.44**	**22.46–36.31**	**40.6–77.9**	**35,459–48,372**	**0.016–0.037**	**879–2118**	**14.83–21.12**	**7.75–9.89**	**89.40–115.41**
Potter Cove											
1994–1995[f]	–	–	–	4.11–8.11	73.4–156.3	5150–21,390	–	790–1130	–	2.29–5.52	44.96–63.02
2004–2005[g]	–	<0.1–0.69	–	4.1–9.8	51–141	6935–36,550	–	525–953	–	3.2–22	41–78
2005–2006[h]	–	0.56–0.69	–	4.2–6.5	54–82	32,800–34,100	–	690–700	–	4.9–5.8	52–63
2010–2012[i]	3.5–14.2	0.093–0.199	10.6–28.2	10.1–25.6	48–155	32,192–78,467	0.009–0.053	617–1109	5.3–13.7	5.6–34.1	42–83
2020[v]	**8.83**	**0.206**	**16.99**	**17.46**	**80.9**	**31,006**	**0.014**	**903**	**8.54**	**7.39**	**73.71**
Deception Island											
1987–1989[j]	20–76	–	24–75	15–88	22–63	–	–	908–1361	10–48	10–16	70–102
2000[k]	17	2	–	9	14	21,600	–	600	6	12	26
2007–2008[l]	–	–	–	11–19	22–42	–	–	695–925	0.9–3.3	–	42–65
2020[v]	**3.15-17.30**	**0.147-0.253**	**18.20–28.98**	**27.91–77.30**	**28.8–39.8**	**31,301–37,886**	**0.017–0.075**	**989–1273**	**14.178–28.05**	**5.49–7.29**	**72.96–90.17**
Central Bransfield Basin											
Date unknown[m]	–	–	16–27	71–86	55–68	–	–	–	26–29	–	91–120
2020[v]	**3.68-11.20**	**0.177-0.284**	**13.64–27.51**	**24.10–45.60**	**38.4–65.9**	**29,088–41,090**	**0.016–0.074**	**652–1280**	**12.468–20.304**	**7.06–13.57**	**74.88–102.11**
Other areas of Antarctica											
Penguin Island[l]	–	–	–	49–82	30–60	–	–	587–670	20–35	–	43–70
Adelaide Island 2006[n]	–	0.1	4.7	2.9	20.7	–	–	211	5.2	2.4	33.8
Adelaide Island 2011[o]	–	0.2–0.5	6.1–10.1	10.0–18.0	19.6–44.3	14,900–26,300	–	212–404	5.8–11.2	4.8–5.0	29.6–54.3
Bellingshausen Sea[p]	–	–	6–11	31–44	16–23	–	–	418–634	13–27	11.4–24.8	72–144
East Amundsen Sea[p]	–	–	9–11	41–54	15–105	–	–	468–564	15–25	18.1–30.6	96–125
West Amundsen Sea[p]	–	–	12–16	44–62	19–48	–	–	542–762	22–28	20.6–33.8	128–179
McMurdo Station[q]	0.83–5.2	0.03–0.46	–	–	0.9–100	–	<0.001–0.087	–	–	0.34–66	17–156
Terra Nova Bay[r]	2.57	0.76	11.20	39.70	67	33,000	–	1180	25.90	10.40	115
Ross Sea[s]	–	0.11–1.64	12.1–19.0	12–115	11.6–33.4	9145–57,550	–	372–1048	10.0–45.7	4.3–36.5	52–130
Windmill Islands[t]	–	0.5–2.5	3.44–4.92	22.0–29.2	13.5–20.0	–	–	–	10.0–14.3	6.0–14	50–70
Weddell Sea[u]	–	–	–	91–146	31–44	–	–	464–660	53–63	–	–

[a] Santos et al. (2005).
[b] Trevizani et al. (2016), Santos et al. (2006).
[c] Santos et al. (2007).
[d] Ribeiro et al. (2011).
[e] Ahn et al. (1996).
[f] Andrade et al. (1999).

[g] Curtosi et al. (2010).
[h] Vodopivez et al. (2015).
[i] Vodopivez et al. (2019).
[j] Somoza et al. (2004).
[k] Deheyn et al. (2005).
[l] Guerra et al. (2011).
[m] Lee et al. (2005).
[n] Grand (2006).
[o] Webb et al. (2020).
[p] Simões et al. (2018).
[q] Negri et al. (2006).
[r] Casalino et al. (2012).
[s] Ianni et al. (2010), Farmer et al. (2006), Burgay et al., 2020.
[t] Gasparon et al. (2007).
[u] Miemistö and Perttilä (1998).
[v] This study.

anthropogenic contamination and the Pb values there were 6 to 7 times higher than those found in uncontaminated sites. Therefore, it can be expected that contaminated sediments would display considerably higher values than found here.

With regard to Cr, our results were consistent with those measured by Santos et al. (2005, 2007) in nearshore surface sediments of Admiralty Bay in 2002–2003 and 2004. However, concentrations of Cr in our study were higher than the ones measured by Ribeiro et al. (2011) in 2006–2007, with values ranging from 31 to 40 μg/g compared to 7–12 μg/g. Our study also found Cr concentrations that were about two times higher than those measured by Trevizani et al. (2016) in 2003. In Potter Cove, values for Cr were also higher in the current study compared to concentrations measured before 2010 (17 μg/g compared to 4.1–9.8 μg/g) but were similar to those measured by Vodopivez et al. (2019) in 2010–2012. Cr levels measured in samples of Collins Bay were three to four times higher than measured in 1993 (22.5–36.3 μg/g in this study compared to 7.6 μg/g). It is therefore interesting to notice that this Cr increase is consistent in all studied sites around KGI. A similar increase in the sediments of Hangar Cove (Adelaïde Island, further south along the Antarctic Peninsula), was measured by Webb et al. (2020) as compared to previous measurements taken at the same location in 2006 by Grand (2006). De Castro-Fernández et al. (2021) also reported increasing Cr concentrations in suspended particulate organic matter (SPOM) and in the red algae *Palmaria decipiens* in the Antarctic Peninsula. Despite being an essential nutrient, Cr is a trace metal that becomes toxic for biota when available in high quantities. The concentrations measured in the northern Antarctic Peninsula are similar to those found at other sites around Antarctica and even much lower than those found in certain parts of the Ross and Weddell Seas. However, although the concentrations do not reach levels of ecological concern yet, this increase in Cr should be monitored in case it is the result of anthropogenic activities (e.g. petroleum contamination). Indeed, most elements showed stable or non-significant trends in Admiralty Bay, Collins Bay and Potter Cove except for Cr for which a significantly increasing trend was found since 1993 ($r = 0.54$, $p < 0.001$). In the area of DI, we generally found higher values of Fe but lower values of As, Cd, Co and Pb than previously measured. The concentrations of Cr, Cu, Mn, Ni and Zn were similar to those measured within the caldera of DI by Somoza et al. (2004) in 1987–1989 but Cr, Ni and Zn were all higher in this study compared to studies from 2000 and 2007–2008. With regards to the CBB, our values were generally consistent with those from Lee et al. (2005), although we had lower concentrations of Cr and Ni.

In conclusion, the results of this study showed a clear distinction between the stations in Hope Bay and the rest of the Bransfield Strait, with lower concentrations of Fe, Mn, Co, V and Zn. On the contrary, the stations around KGI were characterised by moderate to significant enrichment in the toxic elements (e.g. As, Cd, Cu, Pb) while stations in the WBB and around DI had higher Cr and Ni concentrations. Our results showed a clear geochemical distinction between these regions, but also demonstrated the presence of high local heterogeneities. This illustrates the need for a more comprehensive sampling and highlights the importance of sharing collected data to enable better monitoring while reducing the redundancy of conducted studies and their impact on the Antarctic environment. To these ends, our study also proved that the use of FP-XRF in a semi-quantitative way in uncontaminated environments is possible since this method showed a good correlation with ICP-MS analyses. Although two stations displayed moderate to heavy As contamination and twelve presented a moderate ecological risk, most elements are believed to originate from natural sources (e.g. erosion or volcanic activities) and our study did not detect any evident sign of anthropogenic pollution. The values reported in this study can therefore be considered as baseline values. However, our findings suggest an increase in Cr consistent with other studies that would be worthwhile investigating further.

CRediT authorship contribution statement

Louise Delhaye: Conceptualization, Investigation, Methodology, Formal analysis, Writing – original draft, Writing – review & editing, Visualization, Project administration, Funding acquisition. **Marc Elskens:** Conceptualization, Resources, Methodology, Supervision, Writing – review & editing. **Constanza Ricaurte-Villota:** Resources, Methodology, Writing – review & editing. **Luis Cerpa:** Writing – review & editing, Project administration. **Marc Kochzius:** Supervision, Writing – review & editing, Funding acquisition.

Declaration of competing interest

The authors declare that they have no known competing financial interests or personal relationships that could have appeared to influence the work reported in this paper.

Data availability

Data are available in the Supplementary Materials.

Acknowledgments

We thank the Directorate of Antarctic Affairs of the Ministry of Foreign Affairs of Peru for the facilities provided to participate in the ORCA Cruise, as well as the Commander of the BAP Carrasco and his body of officers and non-commissioned officers for their support and willingness to take samples. We also thank the BAP Carrasco crew and researchers from the second leg of the ANTARXXVII campaign (2020) for their support on board in the collection of the samples for this study. The authors also thank BELSPO, VLIR-UOS, the VUB and the Royal Belgian Institute of Natural Sciences for their financial and logistical contribution, enabling the participation in the campaign and the analyses of the data. Special thanks to INVEMAR for the financial support to Constanza Ricaurte-Villota. Finally, the authors thank the researchers Isabelle Schön, Silvio Andrés Ordoñez and Magnolia Murcia for their collaboration in logistics, field work and FP-XRF measurements.

Funding

This work was supported by the Belgian Science Policy Office (BELSPO), the Directorate of Antarctic Affairs of the Ministry of Foreign Affairs of Peru and a VLIR-UOS travel grant.

Appendix A. Supplementary data

Supplementary data to this article can be found online at https://doi.org/10.1016/j.marpolbul.2022.114501.

References

Ahn, I.-Y., Lee, S.H., Kim, K.T., Shim, J.H., Kim, D.-Y., 1996. Baseline heavy metal concentrations in the Antarctic clam, laternula elliptica in Maxwell Bay, King George Island, Antarctica. Mar. Pollut. Bull. 32, 592–598.

Ahn, I.-Y., Ho, Chung K., Choi, H.J., 2004. Influence of glacial runoff on baseline metal accumulation in the Antarctic limpet nacella concinna from King George Island. Mar. Pollut. Bull. 49, 119–141.

Ammann, A.A., 2007. Inductively coupled plasma mass spectrometry (ICP-MS): a versatile tool. J. Mass Spectrom. 42, 419–427.

Andrade, S., Poblet, A., Scagliola, M., Vodopivez, C., Curtosi, A., Pucci, A., Marcovecchio, J., 1999. « distribution of heavy metals in surface sediments from an Antarctic marine ecosystem". Environ. Monit. Assess. 66, 147–158.

Barbieri, M., 2016. The importance of enrichment factor (EF) and geoaccumulation index (Igeo) to evaluate the soil contamination. J. Geol. Geophys. 5 (1), 237. https://doi.org/10.4172/2381-8719.1000237.

Barbosa, Silva A., Arigony-Neto, J., Holger, Braun M., Almeida Espinoza, J.M., Costi, J., Jaña, R., 2020. Spatial and temporal analysis of changes in the glaciers of the Antarctic peninsula. Glob. Planet. Chang. 184, 103079.

Bárcena, M.A., Isla, E., Plaza, A., Flores, J.A., Sierro, F.J., Masqué, P., Sanchez-Cabeza, J. A., Palanques, A., 2002. Bioaccumulation record and paleoclimatic significance in the Western Bransfield Strait. The last 2000 years. Deep-Sea Res. II 49, 935–950.

Bargagli, R., 2000. Trace metals in Antarctica related to climate change and increasing human impact. Rev. Environ. Contam. Toxicol. 166, 129–173.

Bargagli, R., 2008. Environmental contamination in Antarctic ecosystems. Sci. Total Environ. 212–226.

Bargagli, R., Nelli, L., Ancora, S., Focardi, S., 1996. Elevated cadmium accumulation in marine organisms from Terra Nova Bay (Antarctica). Polar Biol. 16, 513–520.

Biryol, C.B., Lee, S.J., Lees, J.M., Shore, M.J., 2018. Lithospheric structure of an incipient rift basin: results from receiver function analysis of Bransfield Strait, NW Antarctic peninsula. Polar Sci. 16, 47–58.

Bosneaga, A., Georgescu, L., Ene, A., 2011. Evaluation of soils pollution with heavy metals using XRF technique. J. Environ. Prot. Ecol. 12 (1247), 1254.

Boutron, C., Candelone, J.-P., Hong, S., 1994. Past and recent changes in the large-scale tropospheric cycles of lead and other heavy metals as documented in Antarctic and Greenland snow and ice: a review. Geochim. Cosmochim. Acta 58, 3217–3225.

Burgay, F., Abollino, O., Buoso, S., Costa, E., Giacomino, A., La Gioia, C., Fraterrigo, Garofalo S., Pecoraro, G., Malandrino, M., 2020. Geochemical characterization of a marine sediment core from the Joides Basin, Ross Sea, Antarctica. Mar. Geol. 428, 106286.

Cabrita, M.T., Padeiro, A., Amaro, E., dos Santos, M.C., Leppe, M., Verkulich, S., Hughes, K.A., Peter, H.-U., Canário, J., 2017. Evaluating trace element bioavailability and potential transfer into marine food chains using immobilized diatom model species Phaeodactylum tricornutum, on King George Island, Antarctica. Mar. Pollut. Bull. 121, 192–200.

Casalino, C.E., Malandrino, M., Giacomino, A., Abollino, O., 2012. Total and fractionation metal contents obtained with sequential extraction procedures in a sediment core from Terra Nova Bay, West Antarctica. Antarct. Sci. 25, 83–98.

Castillo, P., Lacassie, J.P., Augustsson, C., Hervé, F., 2014. Petrography and geochemistry of the carboniferous-triassic trinity peninsula group, West Antarctica: implications for provenance and tectonic setting. Geol. Mag. 152, 575–588.

Curtosi, A., Pelletier, E., Vodopivez, C., St, Louis R., Cormack, W., 2010. « presence and distribution of persistent toxic substances in sediments and marine organisms of potter cove, Antarctica". Arch. Environ. Contam. Toxicol. 59, 582–592.

Daszykowski, K., Kaczmarek, Y.Vander, Heyden, B.Walczak, 2007. Robust statistics in data analysis — a review basic concepts. Chemom. Intell. Lab. Syst. 85, 203–219.

De Castro-Fernández, P., Cardona, L., Avila, C., 2021. Distribution of trace elements in benthic infralittoral organisms from the western Antarctic peninsula reveals no latitudinal gradient of pollution. Sci. Rep. 11, 16266.

Deheyn, D.D., Gendreau, P., Baldwin, R.J., Latz, M.I., 2005. Evidence for enhanced bioavailability of trace elements in the marine ecosystem of Deception Island, a volcano in Antarctica. Mar. Environ. Res. 60, 1–33.

Drake, L., 2014. Core Analysis With the Tracer. Bruker Elemental.

Farías, S., Smichowski, P., Vélez, D., Montoro, R., Curtosi, A., Vodopívez, C., 2007. Total and inorganic arsenic in Antarctic macroalgae. Chemosphere 69, 1017–1024.

Farmer, G.L., Licht, K., Swope, R.J., Andrews, J., 2006. Isotopic constraints on the provenance of fine-grained sediment in LGM tills from the Ross embayment, Antarctica. Earth Planet. Sci. Lett. 249, 90–107.

Gao, Y., De Brauwere, A., Elskens, M., Croes, K., Baeyens, W., Leermakers, M., 2013. Evolution of trace metal and organic pollutant concentrations in the Scheldt River Basin and the Belgian Coastal Zone over the last three decades. J. Mar. Syst. 128, 52–61. December 2013.

Gasparon, M., Matschullat, J., 2006. Trace metals in Antarctic ecosystems: results from the Larseman Hills, East Antarctica. Appl. Geochem. 21, 1593–1612.

Gasparon, M., Ehrler, K., Matschullat, J., Melles, M., 2007. Temporal and spatial variability of geochemical backgrounds in the Windmill Islands, East Antarctica: implications for climatic changes and human impacts. Appl. Geochem. 22, 888–905.

Gordon, A.L., Nowlin Jr., W.D., 1977. The basin waters of the Bransfield Strait. J. Phys. Oceanogr. 8, 258–264.

Grand, M.M., 2006. Evidence for Meltwater Influence on Heavy Metal Accumulation in the Antarctic Lipet Nacella Concinna in Coastal Waters off Rothera Station, Antarctica. University of Plymouth. M.Sc. Thesis.

Guerra, R., Fetter, E., Ceschim, L.M.M., Martins, C.C., 2011. Trace metals in sediment cores from deception and Pingouin Islands (South Shetland Islands, Antarctica). Mar. Pollut. Bull. 62, 2571–2575.

Hakanson, L., 1979. An ecological risk index for aquatic pollution control. A sedimentological approach. Water Res. 14, 975–1001.

IAEA, 2005. In Situ Applications of X-Ray Fluorescence Techniques.

Ianni, C., Magi, E., Soggia, F., Rivaro, P., Frache, R., 2010. Trace metal speciation in coastal and off-shore sediments from Ross Sea (Antarctica). Microchem. J. 96, 203–212.

Islam, Md.S., Tanaka, M., 2004. Impacts of pollution on coastal and marine ecosystems including coastal and marine fisheries and approach for management: a review and synthesis. Mar. Pollut. Bull. 48, 624–649.

Keller, R.A., Fisk, M.R., White, W.M., Birkenmajer, K., 1991. Isotopic and trace element constraints on mixing and melting models of marginal basin volcanism, Bransfield Strait, Antarctica. Earth Planet. Sci. Lett. 111, 287–303.

Kuerban, M., Maihemuti, B., Waili, Y., Tuerhong, T., 2020. Ecological risk assessment and source identification of heavy metal pollution in vegetable bases or urumqi, China, using the positive matrix factorization (PMF) method. PLOS ONE 15 (4), e0230191.

Lee, J.I., Park, B.-K., Jwa, Y.-J., Yoon, H.I., Yoo, K.C., Kim, Y., 2005. Geochemical characteristics and the provenance of sediments in the Bransfield Strait, West Antarctica. Mar. Geol. 219, 81–98.

Lee, S., Kim, S.-J., Ju, S.-J., Pak, S.-J., Son, S.-K., Yang, J., Han, S., 2015. Mercury accumulation in hydrothermal vent mollusks from the southern Tonga arc, southwestern Pacific Ocean. Chemosphere 127, 246–253.
Masqué, P., Isla, E., Sanchez-Cabeza, J.A., Palanques, A., Bruach, J.M., Puig, P., Guillén, J., 2002. Sediment accumulation rates and carbon fluxes to bottom sediments at the Western Bransfield Strait (Antarctica). Deep-Sea Res. II 49, 921–933.
Miemistö, L., Perttilä, 1998. Trace elements in the Weddell Sea water and sediments in the continental shelf area. Chemosphere 31, 3643–3650.
Negri, A., Burns, K., Boyle, S., Brinkman, D., Webster, N., 2006. Contamination in sediments, bivalves and sponges of McMurdo Sound, Antarctica. Environ. Pollut. 143, 456–467.
Potapowicz, J., Szumińska, D., Szopińska, M., Bialik, R.J., Machowiak, K., Chmiel, S., Polkowska, Z., 2020. Seashore sediment and water chemistry at the Admiralty Bay (King George Island, maritime Antarctica) - geochemical analysis and correlations between the concentrations of chemical species. Mar. Pollut. Bull. 152, 110888.
Reed, S., Clark, M., Thompson, R., Hughes, K.A., 2018. Microplastics in marine sediments near Rothera Research Station, Antarctica. Mar. Pollut. Bull. 133, 460–463.
Ribeiro, A.P., Figueira, R.C.L., Martins, C.C., Silva, C.R.A., França, E.J., Bícego, M.C., Mahiques, M.M., Montone, R.C., 2011. Arsenic and trace metal contents in sediment profiles from the Admiralty Bay, King George Island, Antarctica. Mar. Pollut. Bull. 62, 192–196.
Santos, I., Silva-Filho, E., Schaefer, C., Albuquerque-Filho, M.R., Campos, L.S., 2005. Heavy metal contamination in coastal sediments and soils near the brazilian Antarctic Station, King George Island. Mar. Pollut. Bull. 50, 185–194.
Santos, I., Silva-Filho, E., Schaefer, C., Sella, S., Silva, C., Gomes, V., Passos, M., Ngan, P., 2006. Baseline mercury and zinc concentrations in terrestrial and coastal organisms of Admiralty Bay, Antarctica. Environ. Pollut. 140, 304–311.
Santos, I., Fávaro, D., Schaefer, C., Silva-Filho, E., 2007. Sediment geochemistry in coastal maritime Antarctica (Admiralty Bay, King George Island): evidence from rare earths and other elements. Mar. Chem. 107, 464–474.
Simões, Pereira P., van de Flierdt, T., Hemming, S.R., Hammond, S.J., Kuhn, G., Brachfeld, S., Doherty, C., Hillenbrand, C.-D., 2018. Geochemical fingerprints of glacially eroded bedrock from West Antarctica: detrital thermochronology, radiogenic isotope systematics and trace element geochemistry in late holocene glacial-marine sediments. Earth Sci. Rev. 182, 204–232.
Smellie, J.L., Pankhurst, R.J., Thomson, M.R.A., Davies, R.E.S., 1984. The geology of the South Shetland Islands: VI. Stratigraphy, geochemistry and evolution. In: British Antarctic Survey, Scientific Reports, No 87.
Somoza, L., Martínez-Frías, J., Smellie, J.L., Rey, J., Maestro, A., 2004. Evidence for hydrothermal venting and sediment volcanism discharged after recent short-lived volcanic eruptions at deception island, Bransfield Strait, Antarctica. Mar. Geol. 203, 119–140.
Suttie, E., Wolff, E., 1993. The local deposition of heavy metal emissions from point sources in Antarctica. Atmos. Environ. 27A (12), 1833–1841.
Thompson, M., Ellison, S.L.R., Wood, R., 2002. Harmonised guidelines for single laboratory validation of methods of analysis. Pure Appl. Chem. 74 (5), 835–855.
Trevizani, T.H., Lopes Figueira, R.C., Ribeiro, A.P., Theophilo, C.Y.S., Pereira Majer, A., Varella Petti, M.A., Corbisier, T.N., Montone, R.C., 2016. Bioaccumulation of heavy metals in marine organisms and sediments from Admiralty Bay, King George Island, Antarctica. Mar. Pollut. Bull. 106, 366–371.
Trevizani, T.H., Varella Petti, M.A., Ribeiro, A.P., Corbisier, T.N., Lopes Figueira, R.C., 2018. Heavy metal concentrations in the benthic trophic web of Martel Inlet, Admiralty Bay (King George Island, Antarctica). Mar. Pollut. Bull. 130, 198–205.
Veny, M., Aguiar-González, B., Marrero-Díaz, A., Rodríguez-Santana, A., 2022. Seasonal circulation and volume transport of the Bransfield current. Prog. Oceanogr. 204, 1–13.
Vodopivez, C., Smichowski, P., Marcovecchio, J., 2001. Trace metals monitoring as a tool for characterization of Antarctic ecosystems and environmental management. The Argentine programme at Jubany Station. In: Environmental Contamination in Antarctica, Chap. 6.
Vodopivez, C., Curtosi, A., Villaamil, E., Smichowski, P., Pelletier, E., Mac Cormack, W. P., 2015. Heavy metals in sediments and soft tissues of the Antarctic clam laternula elliptica: more evidence as a possible biomonitor of coastal marine pollution at high latitudes? Sci. Total Environ. 502, 375–384.
Vodopivez, C., Curtosi, A., Pelletier, E., Spairani, L.U., Hernández, E.A., Mac Cormack, W.P., 2019. Element concentrations of environmental concern in surface sediment samples from a broad marine area of 25 de Mayo (King George) island, South Shetland Islands. Sci. Total Environ. 646, 757–769.
Webb, A.I., Hughes, K.A., Grand, M.M., Lohan, M.C., PeckI, S., 2020. Sources of elevated heavy metal concentrations in sediments and benthic marine invertebrates of the western Antarctic peninsula. Sci. Total Environ. 698.
Wedepohl, H., 1995. The composition of the continental crust. Geochim. Cosmochim. Acta 59, 1217–1232.